Table 1 Flow properties

Stagnation enthalpy, MJ/kg	Mach number	Static pressure, kPa	Pitot pressure, kPa	Static temperature, K	Flow velocity, km/s	Density, kg/m^3
14.9	5.2	18	580	2000	4.6	0.029

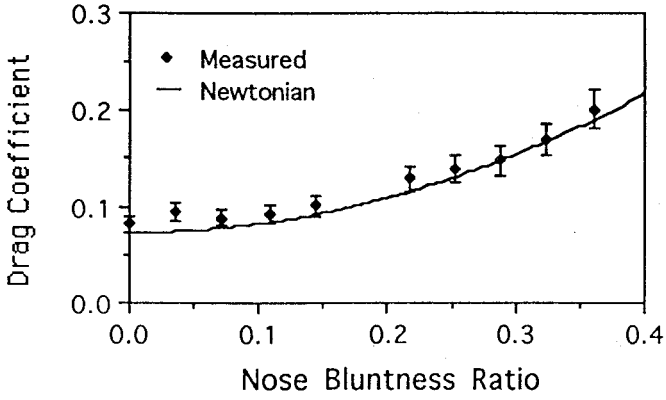

Fig. 2 Drag coefficient vs bluntness ratio from both the measured results and the Newtonian prediction.

constant throughout the test time. The driver gas composition was 90% helium and 10% argon.

The conditions in the test section were numerically determined using ESTC[5] and NENZF.[6] The shock speed in the shock tube, the shock tube fill pressure, and the stagnation pressure were measured and used as inputs to ESTC to determine the temperature of the test gas in the stagnation region after shock reflection. The test gas undergoes a steady expansion from the stagnation region to the test flow properties at the exit plane of the nozzle. NENZF is a one-dimensional nonequilibrium code which predicts the properties of the test gas at the exit plane of the nozzle given the stagnation pressure and temperature. Experiments were performed in a test gas of air at a freestream Mach number of 5.2 and a stagnation enthalpy of 14.9 MJ/kg. A summary of the test flow properties is shown in Table 1. This condition corresponds to an equivalent flight speed of approximately 5.5 km/s.

Results and Discussion

The strain gauge signal was deconvoluted numerically as described previously to obtain the time history of the drag on the model. This drag measurement technique is inherently noisy as the deconvolution process tends to amplify any noise present in the original output signal $y(t)$. Thus, it was necessary to pass all of the drag measurements resulting from the numerical deconvolution process through a 2-kHz, 6-pole Butterworth low-pass digital filter. Figure 1 shows an example of the measured drag after filtering in comparison with its corresponding strain gauge output signal before deconvolution. An estimate of the accuracy of the technique indicates values are correct to $\pm 10\%$.

The results are summarized in Fig. 2 in a plot of drag coefficient vs nose bluntness ratio. At the smaller nose bluntnesses the effect of nose bluntness on the total drag is small. There is an increase in drag from the sharp nose value of only about 20% at a bluntness ratio of 0.144 (nose radius of 7.2 mm). Beyond this bluntness ratio, however, the drag increases more rapidly so that at a bluntness ratio of 0.36 (nose radius of 18.0 mm) the value of drag is about 145% greater than the drag on the sharp cone.

The Newtonian sine-square law[7] was used to obtain an approximation of the pressure coefficient on the cone. The Newtonian law modified for blunted bodies[7] was used to estimate the pressure coefficient over the blunted nose region. The drag coefficient was calculated based on these approximations and is also plotted in Fig. 2. There is good agreement between the measured drag coefficients and the Newtonian predictions. This would indicate the absence of any real gas effects on blunted cone drag in this hypervelocity flow. This is in agreement with blunted cone studies made in a hypervelocity ballistic range.[3]

Conclusions

The results indicate that, for small cone angles, the drag of a blunt cone in a hypervelocity flow is reasonably well predicted by the Newtonian sine-square law modified for blunt bodies. This suggests the absence of any real gas effects on the total drag on a blunted slender cone in hypervelocity flow.

The effect of nose bluntness at the smaller bluntness ratios is relatively small, with about a 20% increase in drag at a bluntness ratio of 0.144. This is encouraging for the design of a hypervelocity space plane or a centerbody for an axisymmetric scramjet where a slightly blunted nose is required to reduce stagnation point heating. Beyond a bluntness ratio of 0.144 the drag increases more rapidly with bluntness.

Acknowledgments

The authors are grateful for the support received from the Australian Research Council under grant AE9032029 and the ARC Queen Elizabeth II Fellowship Scheme (for D. J. Mee).

References

[1]Stalker, R. J., and Morgan, R. G., "The University of Queensland Free Piston Shock Tunnel T4—Initial Operation and Preliminary Calibration," NASA CR-181721, Sept. 1988.

[2]Sanderson, S. R., and Simmons, J. M., "Drag Balance for Hypervelocity Impulse Facilities," *AIAA Journal*, Vol. 29, No. 12, 1991, pp. 2185–2191.

[3]Welsh, C. J., Lawrence, W. R., and Watt, R. M., "Real Gas Effects on the Aerodynamics of Blunt Cones as Measured in a Hypervelocity Range," AIAA Paper 80-0373, Jan. 1980.

[4]Sanderson, S. R., Simmons, J. M., and Tuttle, S. L., "A Drag Measurement Technique for Free Piston Shock Tunnels," AIAA Paper 91-0549, Jan. 1991.

[5]McIntosh, M. K., "Computer Program for the Numerical Calculation of Frozen and Equilibrium Conditions in Shock Tunnels," Dept. of Physics, Australian National University, Canberra, Australia, 1968.

[6]Lordi, J. A., Mates, R. E., and Moselle, J. R., "Computer Program for Numerical Solution of Nonequilibrium Expansion of Reacting Gas Mixtures," NASA CR-472, 1966.

[7]Anderson, J. D., *Hypersonic and High Temperature Gas Dynamics*, McGraw-Hill, New York, 1989, pp. 46–56.

Enhanced Mixing of Multiple Supersonic Rectangular Jets by Synchronized Screech

R. Taghavi*
University of Kansas, Lawrence, Kansas 66045
and
G. Raman†
NYMA, Inc., Brook Park, Ohio 44142

Introduction

THERE have been several investigations of screech tones in underexpanded jets. It was shown by Glass[1] and Krothapalli et al.[2]

Received April 16, 1994; revision received June 3, 1994; accepted for publication June 11, 1994; presented as Paper 94-2325 at the AIAA 25th Fluid Dynamics Conference, Colorado Springs, CO, June 20–23, 1994.

*Assistant Professor, Department of Aerospace Engineering. Senior Member AIAA.

†Senior Research Engineer, NASA Lewis Research Center Group, Experimental Fluid Dynamics Section, Cleveland, OH 44135. Member AIAA.

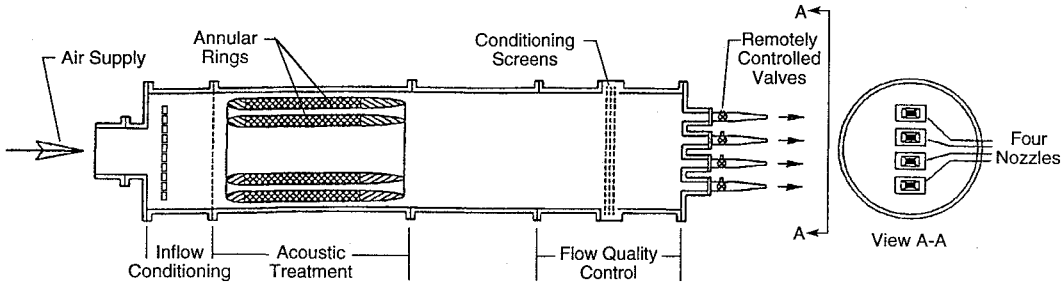

Fig. 1 Schematic of the supersonic jet flow facility.

that screeching jets have spreading rates that are higher than their nonscreeching counterparts. Thus, the idea of using an excitation source such as jet screech that requires no external power seems attractive for jet mixing and noise control applications. Further, in cases where natural screech does not exist, it is possible to induce a screech-like tone using the edge tone concept. A demonstration experiment on "induced screech" was conducted by Rice and Raman[3] using square obstacles that were partially immersed into a supersonic jet. The result was enhanced jet mixing with a severe thrust penalty (20%) due to the drag on the obstacles. This thrust loss can be reduced by proper shaping of the obstacles.[4] The idea of using acoustic feedback from natural or induced screech sources with potential applications in the design of jet mixer noise suppressors was described by Rice.[5]

The potential for the use of multiple jets for enhanced mixing, improved ejector efficiency, and noise control has prompted several other investigations. Krothapalli et al.[6] and Chandrasekhara et al.[7] have conducted extensive studies on a linear array of multiple subsonic and supersonic rectangular jets in an ejector.

The objective of the present work was to study the mixing characteristics of a linear array of supersonic rectangular jets under conditions of screech synchronization. The screech synchronization at a fully expanded jet Mach number of 1.61 was achieved by a precise adjustment of the internozzle spacing. To our knowledge, such an experiment on the resonant mixing of screech synchronized multiple rectangular jets has not been reported before. The results are compared with the case where the screech was suppressed in the multijet configuration.

Experimental Apparatus and Procedure

The existing jet facility at NASA Lewis Research Center was modified with the addition of four identical convergent rectangular nozzles. A schematic drawing of the flow facility is shown in Fig. 1. The exit dimensions of each rectangular nozzle were 6.9 × 34.5 mm (aspect ratio = 5). These nozzles were used to produce four parallel underexpanded jets at a fully expanded Mach number of 1.61. The individual nozzle total pressures could be maintained to within ±0.1 psi by remote control valves.

The frequency and phase difference of the screech tone between adjacent jets were measured by analyzing pairs of signals from four 0.64-cm (B&K) microphones using a 2-channel (B&K) signal analyzer. The microphones were secured to the bottom of each nozzle. The total pressures in the jet flowfield were mapped using a total pressure probe with an o.d. of 0.8 mm.

Two complete sets of experiments were conducted in this study. The first set involved the study of the mixing characteristics of the four underexpanded rectangular jets with synchronized screech. This was accomplished by a precise adjustment of the spacing between the nozzles. The process of changing the internozzle spacing to obtain synchronized screech was done meticulously to ensure that the nozzle alignment was undisturbed. At a fully expanded Mach number of 1.61, an average nozzle spacing of $s/h = 9.084$, provided a screech tone frequency of 6748 Hz for all four jets and screech amplitudes of 163.4, 161.9, 159.1, and 160.6 dB for jets 1–4, respectively (where s is the center-to-center nozzle spacing and h the width of the rectangular nozzle exit). It is important to note that the internozzle spacing was not exactly the same from nozzle to nozzle. The spacings were $s/h = 9.037$ (between 1 and 2),

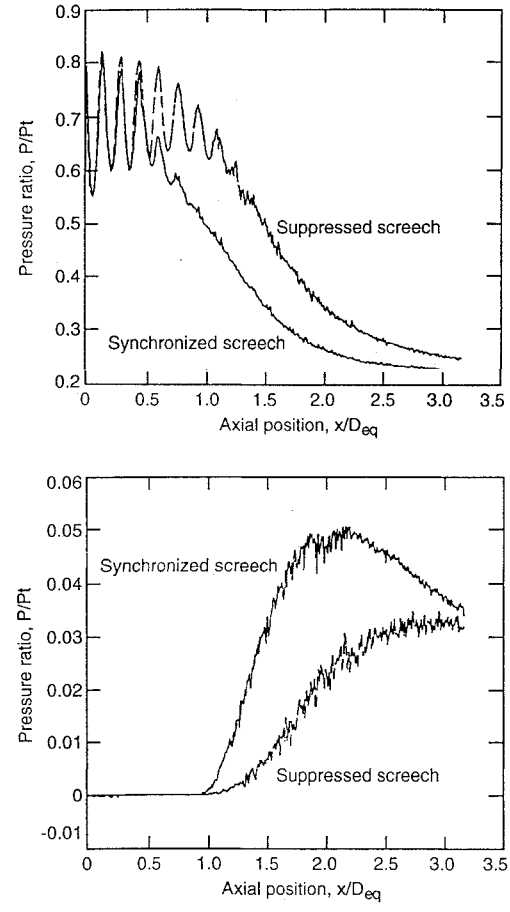

Fig. 2 Typical streamwise distributions of normalized total pressure for the synchronized and suppressed screech cases; P and P_t are the pitot pressure and plenum pressure, respectively: a) centerline of jet 4 and b) between jets 3 and 4.

9.173 (between 2 and 3), and 9.041 (between 3 and 4). The phase difference obtained from the cross spectrum between signals from microphones on adjacent nozzles was 9.7 deg (between 1 and 2), −9.1 deg (between 2 and 3), and 1.6 deg (between 3 and 4) with a measurement accuracy of ±5 deg. The total pressure field was mapped by a pitot tube traversing at various axial stations under computer control.

The second set of experiments involved measurements similar to the first one except that the screech tone amplitude was suppressed and the synchronization was lost. This was accomplished by cancellation of the screech tone near the nozzle lip by installation of a reflecting baffle upstream of the nozzle exit plane. The screech cancellation technique used in these experiments was similar to that reported by Nagel et al.[8] The suppressed screech amplitudes were 143.8, 150.1, 151, and 151.5 dB for jets 1–4, respectively. The phase difference obtained from the cross spectrum between signals from microphones on adjacent nozzles was 104.4 deg (between 1 and 2), 100.4 deg (between 2 and 3), and −59.4 deg (between 3 and 4), with

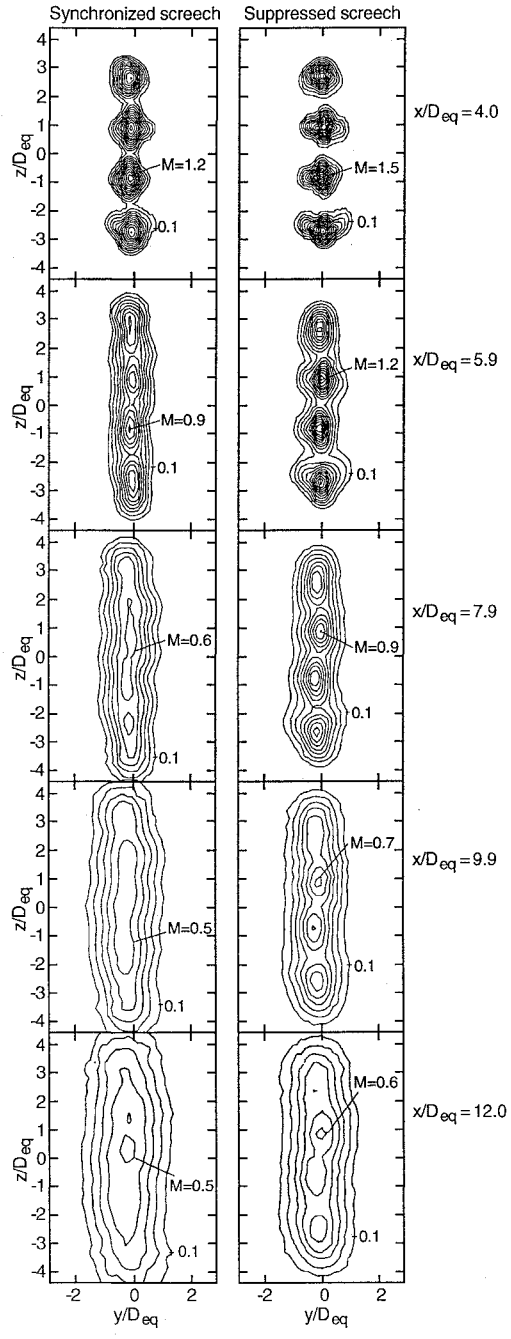

Fig. 3 Mach number contours for synchronized screech and suppressed screech cases; M_j = 1.61; contour interval at 0.1 with x being the streamwise direction and y and z being the directions that are perpendicular to the smaller and larger nozzle dimensions, respectively.

a measurement accuracy of ±5 deg. Therefore, the screech tones in the suppressed screech case were not synchronized.

Results and Discussion

Typical axial variations of normalized pitot pressure, on the jet centerline, for one of the four jets, for both the screech synchronized and suppressed cases are compared in Fig. 2a. It is seen that in the synchronized screech case, the potential core length and the number of shock cells have been reduced to half of that for the suppressed screech case. As a consequence, the centerline pitot pressure at $x/D_{eq} = 1.5$ for the screech synchronized case is only 68% of that for the screech suppressed case. Note that x is the axial distance along the jet centerline, and D_{eq} is the equivalent circular diameter defined as the diameter of a circle having an area (A_e) equal to the total exit area of the four nozzles (i.e., $D_{eq} = \sqrt{(4A_e)/\pi}$). This reduction in centerline pitot pressure for the screech synchronized case is indicative of substantial mixing enhancement, a result

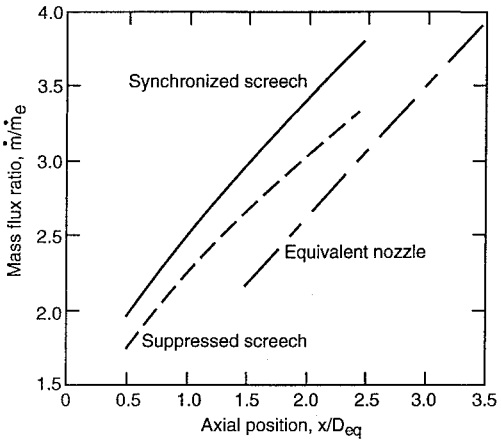

Fig. 4 Variation of normalized mass flux with axial distance for the synchronized and suppressed screech cases; $\dot{m}$ and $\dot{m}_e$ represent the mass flux at various downstream stations and at the nozzle exit, respectively.

that was verified further by computing the mass flux from detailed flowfield data.

Streamwise distributions of the normalized pitot pressure midway between adjacent nozzles are compared in Fig. 2b for one of the four jets for both the screech synchronized and suppressed cases. It needs to be emphasized that midway between the nozzles, immediately downstream of the exit, there is no flow except that due to the mobilization of air due to entrainment by the jets. However, as the pitot tube is moved farther downstream it senses higher pressures due to jet spreading and the initiation of interaction between jets. It is clear from Fig. 2b that the initiation of interjet mixing for the screech synchronized case occurs $0.25D_{eq}$ upstream, more rapidly (higher slope), and also peaks $0.75D_{eq}$ upstream as compared to the screech suppressed case. In addition it should be noted that the maximum value is 65% higher for the screech synchronized case as compared to that for the screech suppressed case.

The Mach number contours are compared for the screech synchronized and suppressed cases in Fig. 3. For stations far downstream, the Mach numbers were subsonic and were obtained from the total pressure data by using isentropic relationships. For these calculations it was assumed that the local static pressure could be approximated by the ambient pressure. For stations closer to the jet exit, the Mach numbers in the core of the jet were supersonic and were calculated using Rayleigh's pitot tube formula. In these calculations it was assumed that the static pressures upstream of the bow shock in front of the pitot probe could be approximated by the ambient pressure. Note that the latter approximation (i.e., for the supersonic Mach numbers) is used only as a qualitative comparison between the various cases. Stations very close to the jet exit ($x/D_{eq} < 4$) have been avoided due to inaccuracies and large measurement uncertainties.

From the data in Fig. 3 it is apparent that the four jets represented by four Mach number islands at $x/D_{eq} = 4$ merge and spread faster for the screech synchronized case than for the screech suppressed case. Note that the Mach number of the center contour and wider contour spacings are indicators of higher jet spread.

The mass-flux ratios for the two cases under consideration are compared in Fig. 4. The data from a single jet emerging from an "equivalent rectangular nozzle" having the same aspect ratio as the individual nozzles and with an exit area equal to the total area of the four nozzles is also included in the figure. The mass-flux ratios were obtained by an integration of the flowfield data over the entire jet cross section. From the data in Fig. 4 it is clear that the screech synchronized multijet case has the highest mass-flux ratio followed by the multijet with suppressed screech, with the single equivalent rectangular jet having the least.

Concluding Remarks

A unique set of data is presented on the effect of synchronized screech on the mixing of a linear array of underexpanded rectangular

jets. Two other cases are provided for comparison. One case is the multijet array with suppressed screech and the other case is a single equivalent rectangular jet with screech. The synchronized screech multijet case produced the maximum mass-flux augmentation followed by the screech suppressed multijet and the screeching single equivalent jet. Future work should focus on investigating synchronized screech excitation for smaller internozzle spacings that are useful for mixer-ejector applications.

Acknowledgments

This research was conducted under Grant NCC-251 from NASA Lewis Research Center. The authors would like to thank John Abbott and Khairul Zaman of NASA Lewis Research Center for their support and technical input to this research. The engineering support of Ralph Fallert and Richard Brokopp (mechanical) and James Little (electronics) is highly appreciated.

References

[1]Glass, D. R., "Effects of Acoustic Feedback on the Spread and Decay of Supersonic Jets," *AIAA Journal*, Vol. 6, No. 10, 1968, pp. 1890–1897.

[2]Krothapalli, A., Hsia, Y., Baganoff, D., and Karamcheti, K., "The Role of Screech Tones in Mixing of an Underexpanded Rectangular Jet," *Journal of Sound and Vibration*, Vol. 106, No. 1, 1986, pp. 119–143.

[3]Rice, E. J., and Raman, G., "Enhanced Mixing of a Rectangular Supersonic Jet by Natural and Induced Screech," AIAA Paper 93-3263, 1993.

[4]Raman, G., and Rice, E. J., "Mixing and Noise Benefit Versus Thrust Penalty in Supersonic Jets Using Impingement Tones," AIAA Paper 94-2955, 1994.

[5]Rice, E. J., "Jet Mixer Noise Suppressor Using Acoustic Feedback," NASA-Lewis Research Center, Patents Pending, Application 08/046, 256, filed April 14, 1993 and 08/194, 654, filed Feb. 10, 1994.

[6]Krothapalli, A., Karamcheti, K., Hsia, Y., and Baganoff, D., "Edge Tones in High-Speed Flows and their Applications to Multiple-Jet Mixing," *AIAA Journal*, Vol. 21, No. 7, 1983, pp. 937,938.

[7]Chandrasekhara, M. S., Krothapalli, A., and Baganoff, D., "Mixing Characteristics of an Underexpanded Multiple Jet Ejector," Stanford Univ., JIAA TR-55, Stanford, CA, 1984.

[8]Nagel, R. T., Denham, H. W., and Papathanasiou, A. G., "Supersonic Jet Screech Tone Cancellation," *AIAA Journal*, Vol. 21, No. 11, 1983, pp. 1541–1545.

Effect of Non-Poisson Samples on Turbulence Spectra from Laser Velocimetry

Dave Sree*
Tuskegee University, Tuskegee, Alabama 36088
and
Scott O. Kjelgaard† and William L. Sellers III†
NASA Langley Research Center, Hampton, Virginia 23681

Introduction

THE estimation of turbulence spectra from "individual realization" laser velocimetry (LV) data is very important in determining the frequency characteristics of turbulent flows and the associated time and length scales of turbulence structure. The turbulence scale information obtained from the spectral estimates can aid in evaluating theoretical and numerical turbulence models. A thorough knowledge of the factors that affect the accuracy of the spectral estimates is essential.

LV data constitute a set of randomly sampled velocity-time data obtained from the light scattered by seed particles passing through the measurement volume. Spectral analysis of such data has been investigated for several years and special techniques are available to obtain the spectral estimates.[1,2] Shapiro and Silverman[3] showed theoretically that alias-free spectral estimates can be obtained if the sampling is Poisson distributed. In applying these techniques to laser velocimetry, it is generally assumed that the particle arrival at the measurement volume is Poisson distributed. Well-controlled LV experiments do exhibit Poisson distributed samples. There are, however, many flow situations where LV data do not show these characteristics, and they deviate from the true Poisson distribution (see Ref. 4). One such "non-Poisson" distribution of samples was encountered by the authors during the axial flow velocity measurements near the reattachment region (about 9-step heights downstream of the step) of a backward-facing step flow facility and is shown in Fig. 1. (A detailed description of the experimental facility, including the LV system, is given in Ref. 4.) Figure 1 shows the probability density function $p(\Delta t)$ of an occurrence of a given interarrival time Δt, displayed on a semilog plot. The variability at large Δt is because of the low number of samples occurring in that range and is typical of an LV experimental observation. The dotted straight line represents the theoretical (Poisson) distribution[4]

$$p(\Delta t) = \nu \exp(-\nu \Delta t)$$

where ν is the mean data rate. A non-Poisson process deviates from this straight line. If the sampling is truly Poisson distributed, then the two curves should overlap.

The problem of non-Poisson sampling is attributed to the complex dynamics of the flow that cause nonhomogeneous distribution of particles in the flow. Sometimes, in the desire to obtain high data rates, one may intentionally try to force a high particle flow rate through the sample volume. This can also cause a nonhomogeneous distribution of seeding and can lead to non-Poisson arrival of data. The effect of non-Poisson sampling on the accuracy of spectral estimates has not been addressed in the literature. This Note presents the results of an investigation into this effect. The study is based on a simulated first-order spectrum, which typifies a one-dimensional turbulence spectrum, and some LV experimental data.

Simulated Data

Generation of both Poisson and non-Poisson distributed samples for a first-order spectrum of the form

$$S(f) = \frac{2}{1 + 10^{-4}(2\pi f)^2}$$

where $S(f)$ is the power spectral density at frequency f, is described in Ref. 4. Non-Poisson distributed Δt were generated at an arbitrary mean data rate of 200 samples/s, by choosing[4]

$$\Delta t_i = [-10 \ln(1 - r_i)/\nu]^2 \qquad i = 1, 2, \ldots$$

where r is a random number between 0 and 1. The probability density function of these Δt is shown in Fig. 2. This Δt distribution closely

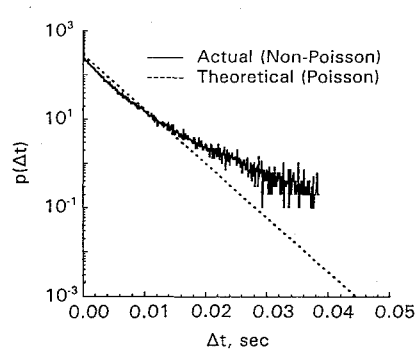

Fig. 1 Probability density function of interarrival times for LV data, ν = 282 samples/s.

Presented as Paper 94-0041 at the AIAA 32nd Aerospace Sciences Meeting and Exhibit, Reno, NV, Jan. 10–13, 1994; received Jan. 20, 1994; revision received May 26, 1994; accepted for publication June 30, 1994.

*Associate Professor, Department of Mechanical Engineering. Member AIAA.

†Aerospace Engineer, Experimental Methods Branch. Member AIAA.